터널과 지하공간, 한국암반공학회지
제18권 제2호, 2008년 4월, pp. 134~148

TUNNEL & UNDERGROUND SPACE, Vol. 18, No. 2, 2008, pp. 134-148
Journal of Korean Society for Rock Mechanics

Effect of Deformation Zones on the State of *In Situ* Stress at a Candidate Site of Geological Repository of Nuclear Waste in Sweden

Ki-Bok Min*

스웨덴 방사성 폐기물 처분장 후보부지의 사례를 통해 살펴본 대규모 변형대가 암반의 초기응력에 미치는 영향

민기복*

Abstract The state of *in situ* stress is an important factor in considering the suitability of a site as a geological repository for nuclear waste. In this study, three-dimensional distinct numerical analysis was conducted to investigate the effect of deformation zones on the state of stress in the Oskarshamn area, which is one of two candidate sites in Sweden. A discontinuum numerical model was constructed by explicitly representing the numerous deformation zones identified from site investigation and far-field tectonic stress was applied in the constructed model. The numerical model successfully captured the variation of measured stress often observed in the rock mass containing large-scale fractures, which shows that numerical analysis can be an effective tool in improving the understanding of the state of stresses. Discrepancies between measured and modelled stress are attributed to the inconsistent quality of measured stress, uncertainty in geological geometry, and input data for fractures.

Key words In situ stress, Deformation zone, Distinct element method, Geological repository of nuclear waste disposal

초 록 암반의 초기응력 상태는 방사성 폐기물 지층 처분장의 적합성을 판단하는데 중요한 요소이다. 본 연구에서는 3차원 개별요소법을 이용하여 스웨덴 방사성 폐기물 처분장 후보지 중 하나인 오스카샴 지역에서 대규모 변형대가 초기응력에 미치는 영향을 살펴보았다. 수치해석에서는 부지조사 과정에서 확인된 변형대를 모델에 포함시켰으며 원거리 지각응력을 경계조건으로 사용하였다. 현지 암반에서 관찰되는 초기응력값의 변화 양상이 수치해석에서도 재현이 됨으로써 수치해석이 암반의 초기응력상태를 이해하는데 유용하게 쓰일 수 있음을 확인하였다. 수치해석을 통한 예측값과 초기응력 측정값과의 차이는 측정된 자료의 양호한 정도, 지질모델 및 변형대의 물성치의 불확실성 등에 기인하는 것으로 생각된다.

핵심어 초기응력, 변형대, 개별요소법, 방사성 폐기물 지층처분장

1. INTRODUCTION

Knowledge of *in situ* stress is critical for the construction of a geological repository for nuclear waste, and *in situ* stress should be taken into account in determining repository site suitability, characterization, and design (Amadei and Stephansson, 1997). One of the difficulties encountered in characterizing *in situ* stress is that it is rarely uniform in a rock mass. The stress distribution in a rock mass can be so complex that local stress may be quite different from average stress (Amadei and Stephansson, 1997). The distributions of *in situ* stresses depend largely on the rock mass structure, including discontinuities and the loads applied to the rock mass throughout its entire geological history. Often, it is difficult to establish precise values for the components of the *in situ* stress.

[1] School of Civil, Environmental and Mining Engineering, University of Adelaide, Australia
* 교신저자 : ki-bok.min@adelaide.edu.au
접수일 : 2008년 4월 10일
심사 완료일 : 2008년 4월 21일

This difficulty has been addressed in a recent collection of state-of-art papers dedicated to 'rock stress' in which the term 'stress estimation' was preferentially used instead of 'stress determination' or 'stress measurement' to emphasize the fact that the measurement of rock stress requires a significant component of 'judgment' or 'opinion' (Hudson and Cornet, 2003; Fairhurst, 2003). Therefore, conscientious efforts are necessary regarding both the accuracy of measured stress and the representation of the measured stress for a region of interest.

Various studies (Pollard and Segall, 1987; Martin and Chandler, 1993; Homberg et al., 1997; Su and Stephansson, 1999) have shown that the existence of fractures can alter the state of stress nearby and that it is important to properly consider the effect of fractures when *in situ* stress is measured. Due to the complexities involved in stress estimation, numerical analysis can be a useful tool to enhance the understanding of rock stress. For point-wise accuracy of stress measurement, numerical modelling can be used for the interpretation of the obtained stress by simulating the transient overcoring process (e.g., Min et al., 2003; Hakala et al., 2003). For the estimation of the global state of stress, numerical modelling can be used to account for the effects of surface topology, excavations, loading history and geological structures on stress state by modelling the region of interest (Hakami et al., 2002; Hart, 2003).

The objective of this paper is to investigate the effect of deformation zones on the measured *in situ* stress at Oskarshamn, Sweden, which is one of the two candidate sites for a geological repository of nuclear waste in Sweden. Measured stresses in the Oskarshamn area are scattered, and it is likely that the large-scale deformation zone identified in the area affects the state of stress. Hence, it is important to understand the mechanisms that influence existing geological structures and to explain with confidence the roles these mechanisms play in the scattered stress values. Attempts have been made to simulate many important large-scale deformation zones that can affect the current state of stress. Furthermore, the modelled state of stress can also provide useful information for the selection of location for the next rock stress measurement campaign.

Despite the usefulness of the two-dimensional numerical study in gaining insights about the problem, a three-dimensional study is necessary to help determine the influence of fracture on the stress state (Hart, 2003). The two-dimensional study can consider either dip or dip direction of fractures, but it cannot model both components of orientation. It is worthwhile to note that the purpose of on-going site characterization is to find a 'volume' of rock that is suitable for the storage of nuclear waste, whereas conventional civil engineering projects, such as the construction of a tunnel, are usually concerned with the state of stress along a 'line'. To understand the state of stress in a volume of rock, three-dimensional numerical analysis was conducted in this study using the three-dimensional distinct element code, 3DEC (Itasca, 2003). Deformation zones obtained from the site investigations were included in the geometry of the numerical model, and far-field boundary stresses are applied in the model to obtain the resulting stress distribution. A comparison was made between the measured stress state *in situ* and the simulated stress state that reflects the influence of large-scale fractures.

2. SITE INVESTIGATION IN SWEDEN AND GEOLOGICAL MODEL

Finding a site that can safely serve as the final repository for nuclear waste is a long, difficult process. While finding such a site is a national issue for many countries, it requires a suitable local solution because it is important that the solution is acceptable to the population located nearby. In Sweden, after feasibility studies conducted in eight municipalities from 1993 to 2000, the Swedish Nuclear Fuel and Waste Management Company (SKB) selected two locations for further investigation based on both technical considerations and local acceptability (Figure 1). Subsequently, SKB has been conducting extensive site investigations in the two selected locations, namely Forsmark and Oskarshamn, since 2003. According to the current plan by SKB, a decision on the final site will be made in 2009, and construction is expected to start early in 2012. A detailed description on the Swedish program for research, development, and methods for the disposal of nuclear waste can be found in SKB (2007). The current study addresses a case study from the Oskarshamn area.

Geological structures at Oskarshamn were characterized through various methods, including out-crop mapping, drill-core mapping, and an extensive geophysical investigation program. The structural model at Oskarshamn consists of a three-dimensional geometrical model of all the major deformation zones and a property table describing the deformation zones. According to the generated map, many deformation zones exist in the Oskarshamn area. Figure 2 shows the geological model and the numerical model of deformation zones at the Oskarshamn site.

Large-scale deformation zones from the geological survey are modelled as planar joints for numerical modelling (Figure 2b). Important borehole locations and reference sections made for analysis are indicated. Section AA' and BB' are parallel with the direction of maximum principal stress and pass through the center and the borehole KAV04 of the local model, respectively. Section CC' passes through the center of the local model and is oriented West- East. Sections DD' and EE' are oriented North-South and pass the boreholes KLX06 and KLX04, respectively. According to the geological survey data, there are more deformation zones inside the local model than outside the local model. This is mainly due to the greater emphasis on characterization in the local model, and comparison of stress should be made in the local model.

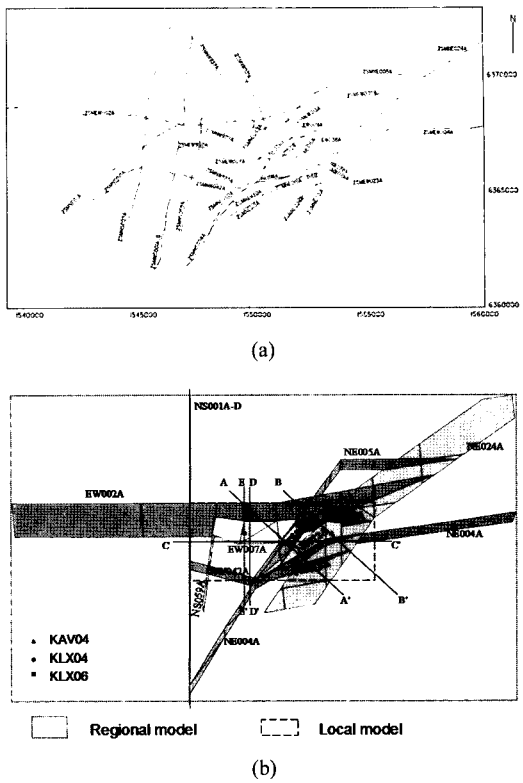

(a)

(b)

Fig. 2. (a) Geological model, (b) numerical model of deformation zones at Oskarshamn Area (SKB, 2006). The sizes of regional and local models are 21 km × 13 km and 7.7 km × 3.2 km, respectively. AA', BB', CC', DD', and EE' denote vertical sections for analysis, and KAV04, KLX04, and KLX06 denote borehole locations

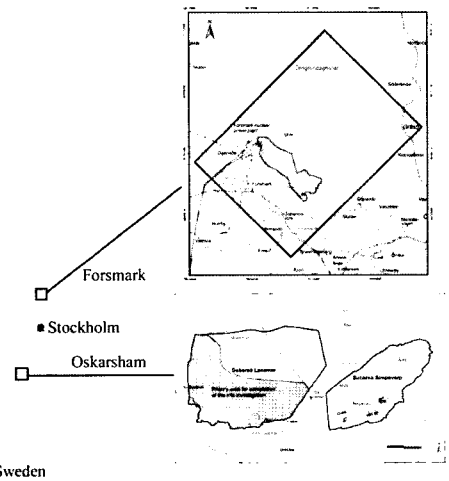

Fig. 1. Locations of two candidate sites in Sweden for a geological repository of nuclear waste (adapted from SKB, 2007)

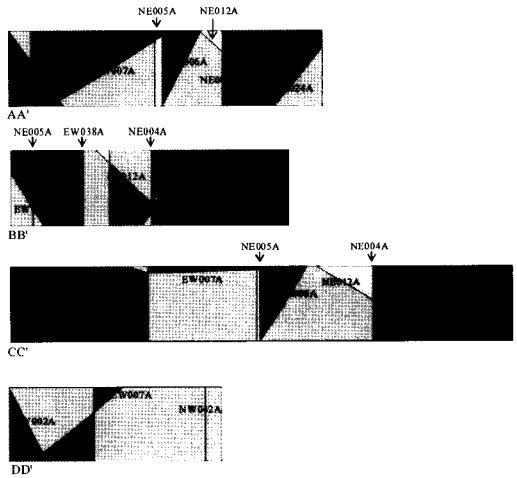

Fig. 3. Vertical section views produced by the local model. The depth of each model is 1.2 km, and the scale of each model can be referred from Figure 2. Section EE' has similar geometry to that of section DD'

The deformation zones that can significantly influence the stress regime are included for the modelling, and the criterion for inclusion is a thickness of 50 m. In certain cases, two narrow-width deformation zones are merged and included in the modelling when they are close and similar in orientation. Figure 3 shows the section views produced by the model along various sections. In the Figure, deformation zone numbers are given and vertical lines without deformation numbers are fictitious joints that were used merely for the construction of the geometry. This does not affect the mechanical behavior of the model. Figure 4 shows horizontal section views of the geometry within the local model. The view changes depending on the depth of the model because of the joints that are not vertical. For example, deformation zone EW002A appears inside the local model with increasing depth, while zone EW007A moves toward the upper boundary of the local model.

3. THREE-DIMENSIONAL DISTINCT ELEMENT MODELLING

The tectonic load acting on the model rock volume is simulated by initiating a major stress in the direction of the overall NW trending tectonic load.

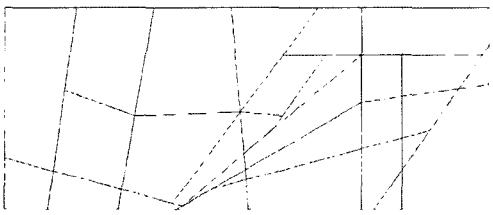

(a) Plan view at the surface

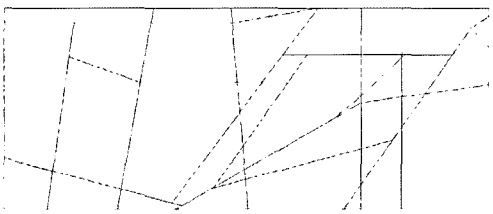

(b) Plan view at the depth of 500 m

Fig. 4. Plan view of geometry generated by the local model in which each line denotes the deformation zone. Compare with the mapped structures at Figure 2

Since the deformation zones are simulated as weak features that may not sustain the applied stress, there may be movements and stress redistribution in the numerical model until an equilibrium state is reached. This equilibrium state is considered as a possible model for the actual distribution in the area, and the results of each model can be compared with the measured stresses until a numerical model is found that gives a reasonable fit. The main mechanism controlling the analysis results is the slip criteria on the fractures, and they are assumed to follow a simple coulomb failure criterion with zero cohesion and a friction angle. Therefore, the friction angle, orientation of fractures, and applied boundary stress are governing factors that control the outcome of the numerical modelling. The credibility of the obtained stress redistribution is based on whether any consistent pattern can be seen in the measurement data (Hakami et al., 2006). Since the detailed characterization of the geological structure is currently on-going, the measured stress data and the input data used in this study involve significant uncertainties. Thus, it is emphasized that the objective of this modelling study is to gain initial insight into the state of stress.

Figure 5 presents the entire geometry of the numerical model with boundary stress conditions. The side lengths of the model are 40 km, and the depth of the model is 4 km. The side of the model is set per-

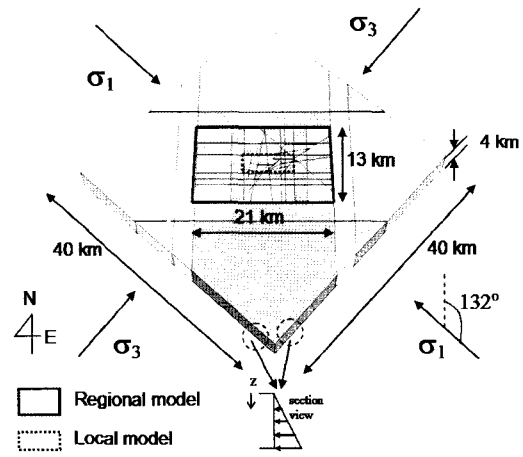

Fig. 5. Geometry of Oskarshamn area modelled by 3DEC. Vertical or horizontal lines shown in the model are fictitious joint and these does not affect the modelling results

pendicular to the direction of principal stress. The regional model, which includes the local model, lies in the center of the model. The boundary stresses are applied with the gradient with increasing depth so that the gradual increase of stress with depth can be modelled properly. The surface of the model is free to move, but displacement of the bottom of the model is confined.

In situ stress obtained from the measurements is used as boundary conditions (SKB, 2004). Horizontal stresses were applied to the lateral boundaries and gravitational stress was imposed within the model. The measured stress data show that the ratio of horizontal stress to vertical stress is about three to four and that the vertical stress is the intermediate principal stress (SKB, 2004). In this study, three stress models (LSMs, Laxemar Stress Models) are used as shown in Figure 6. In order to verify the numerical model used for this study, a square model containing a closed, single fracture was subjected to a biaxial stress, and the resultant shear displacement within the fracture was compared to the available analytical solution. Analytical solution for relative shear displacement (Δu) within a fracture is given as (Pollard and Segall, 1987);

$$\Delta u = (\tau^r - \tau^c)\frac{2(1-\nu)}{G}(a^2 - x^2)^{1/2} \quad (1)$$

where τ^r is remote shear stress; τ^c is shear stress on the crack (fracture); ν is Poisson's ratio; G is shear modulus; a is a half crack length; and x is the distance from the center of a crack. For this verification study, remote shear stress was 20 MPa without shear stress on the crack, Poisson's ratio was 0.25, shear modulus was 20 GPa and half crack length was 2.44 m. As is shown in Figure 7, numerical and analytical solutions reach a perfect agreement. Note that the comparison was made with the friction angle of zero under plane strain condition which is a requirement for the analytical solution.

Figure 8 shows the generated meshes for the model. Finer meshes were used in the region of interest and coarser meshes were used outside of the regional model. The maximum mesh size in the outer model is 2 km, and this is gradually decreased to 0.1 km in the center of the model.

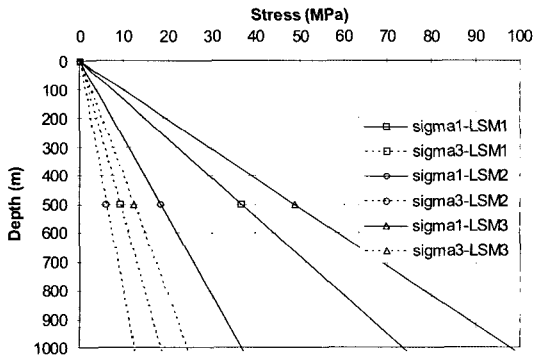

Fig. 6. Three stress models (Laxemar Stress Models) used in the numerical modelling. Note that the gravitational vertical stress is taken as the intermediate principal stress and the major principal stresses LSM1, LSM2, and LSM3 are 3, 1.5, and 4 times gravitational stress, respectively

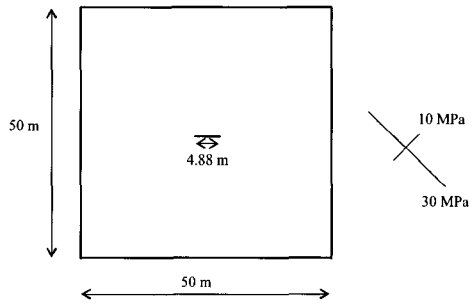

(a)

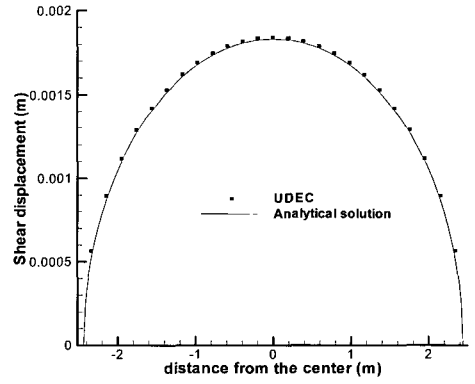

(b)

Fig. 7. Verification of numerical model. (a) geometrical model and boundary condition and (b) comparison of displacement in the a fracture between analytical and numerical solutions

Boundary stresses for the study are listed in Table 1. LSM3 has the largest stress magnitude and the largest stress ratio between maximum and minimum principal stresses, while LSM 2 has the lowest magnitude and the lowest stress ratio. Hence, LSM3 is expected to provide a more optimal condition for the slip of the fracture, which will result in greater effect on stress distribution. Young's modulus and Poisson's ratio for rock masses used in this study were 40 GPa and 0.15, respectively (SKB; 2004). Friction angle is the most important parameter when the effect of discontinuous joint is considered for stress distribution. Friction angle for this study is inferred from existing data on the deformation zone and for small-scale fractures. The measured friction angle of a single fracture ranges from 30 to 40 degrees, and empirical studies suggest that the internal friction angle of the deformation zone is in the order of 40 degrees (SKB, 2004). In this study, a reduced value of 20 degrees was used for the friction angle of fractures. This reduction is justified because larger fractures have smaller friction angles than laboratory-scale fractures, and pore pressure, which allows failure at lower friction angles, was not considered in this study. Discussion of the selection of friction angle for modelling deformation zones as planar joint is presented later.

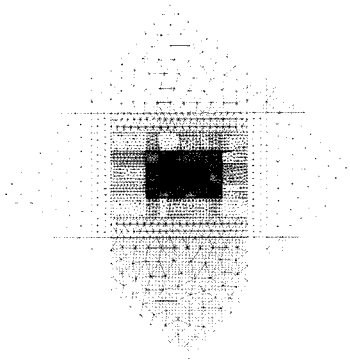

(a)

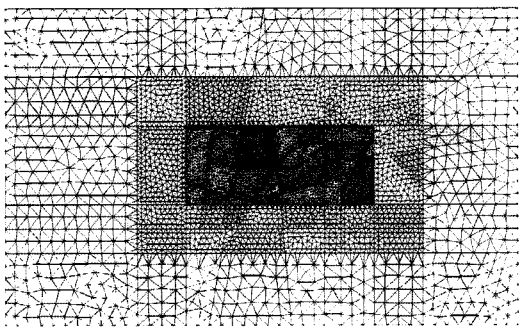

(b)

Fig. 8. Generated meshes for (a) entire model (40 km × 40 km × 4 km) and (b) regional model (21 km × 13 km × 2 km). Average edge length of mesh for the local model was 0.1 km

Normal stiffness of a planar joint that models the deformation zone is 1 GPa/m, and this was determined by estimating the displacement of deformation zones with a width of 50 m. While shear stiffness of the planar joint is assumed to be similar, it would have been more reasonable to assign shear stiffness as 10-20% of normal stiffness (Bandis et al., 1983). However, this does not influence the result of this study because the elastic deformation along the joint does not affect the stress distribution significantly along the joint. In order to consider the simplification of deformation zone NS001A-D, a higher friction angle of 35 degrees and a higher stiffness of 10 GPa/m were assigned for this deformation zone, since sliding along this deformation zone is not expected.

4. MODELLED STATE OF STRESS

The state of stress in the area is presented in various vertical and horizontal sections focusing on

Table 1. Boundary conditions, geometry, and parameters used for the study. The symbol ρ is the density of rock, g is gravitational acceleration, and z denotes the depth

	LSM 1	LSM 2	LSM 3
Maximum Principal stress, σ_1 (MPa)	3 × ρgz	3/2 × ρgz	4 × ρgz
Intermediate Principal stress, σ_2 (MPa)	ρgz	ρgz	ρgz
Minimum Principal stress, σ_3 (MPa)	3/4 × ρgz	1/2 × ρgz	ρgz

the best stress model in order to compare with the measured stress data. Further, the prediction of the stress in a specified borehole and selection of a location for the next measurement campaign are presented.

4.1 Comparison between measured and modelled stress

Measured and modelled stresses in boreholes KLX04 and KAV04 in the Äspö area were compared. Borehole KLX04 is located in the mid-west of the local model (Figure 2), and rock stress was measured by the overcoring method. Borehole intersects the deformation zone EW007A between 314 m and 391 m. The effect of the deformation zone is apparent from the sudden change of measured stress around the location. Figure 9 shows the stress distribution at section EE' for three stress models. Section EE' passes the KLX04 and its location is indicated in the figure. A significant influence of deformation zone EW007A can be observed in LSM 1 and LSM 3. In LSM 2, the effect of deformation zone is not noticeable since sliding of the joint did not occur and, therefore, the stress is not redistributed. In LSM 1 and LSM 3, the wedge formed by EW007A and EW002A has lower stress than other areas. This distinct change of stress is clearer for LSM 3 than LSM 1 because LSM 3 is more favorable for the sliding of the joint, and this induces a greater influence of the deformation zone. Figure 10 presents the comparison between measured and modelled stresses at KLX04. Measured stress shows a distinct increase of stress for maximum and intermediate principal stresses. This is explained by the effect of deformation zone EW007A. Of the three stress models, LSM3 matches best with the measured results.

Borehole KAV04 is located in the mid-east of the

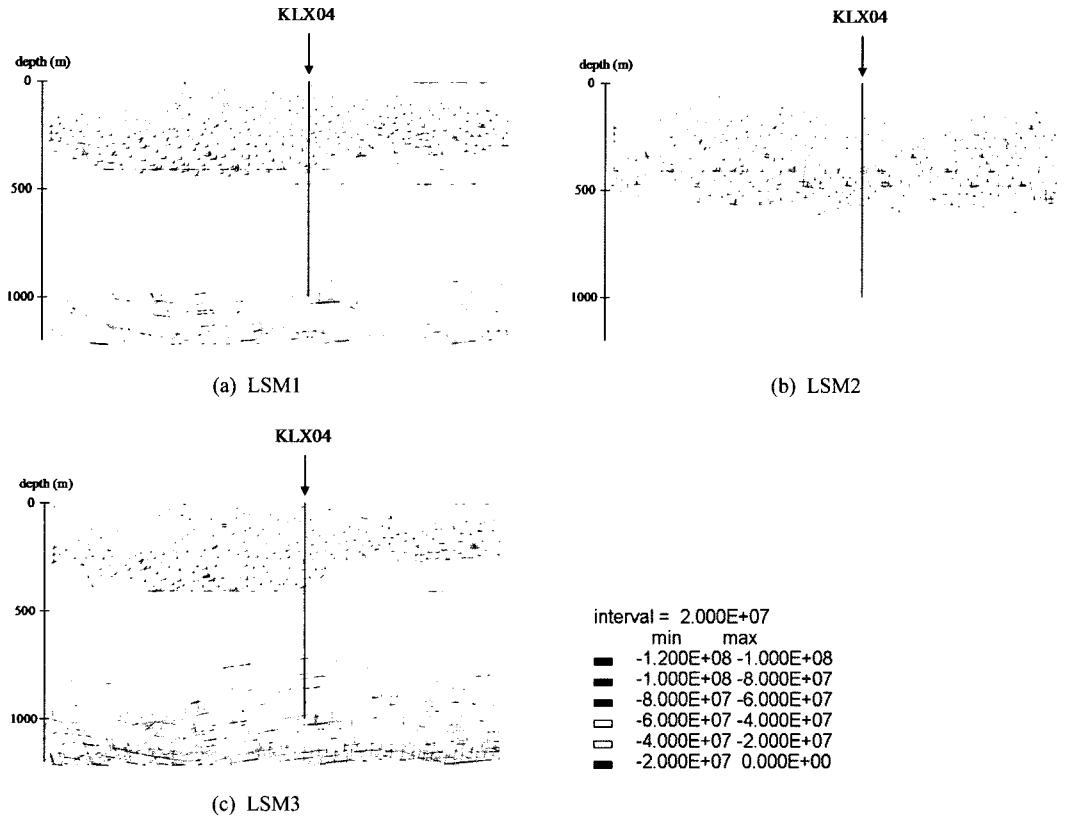

Fig. 9. Stress distribution at Section EE' across borehole KLX04 at (a) LSM1; (b) LSM2; and (c) LSM3. LSM3 model shows most dramatic change of stress. Note that two inclined lines are deformation zones (EW002A and EW007A) forming a wedge

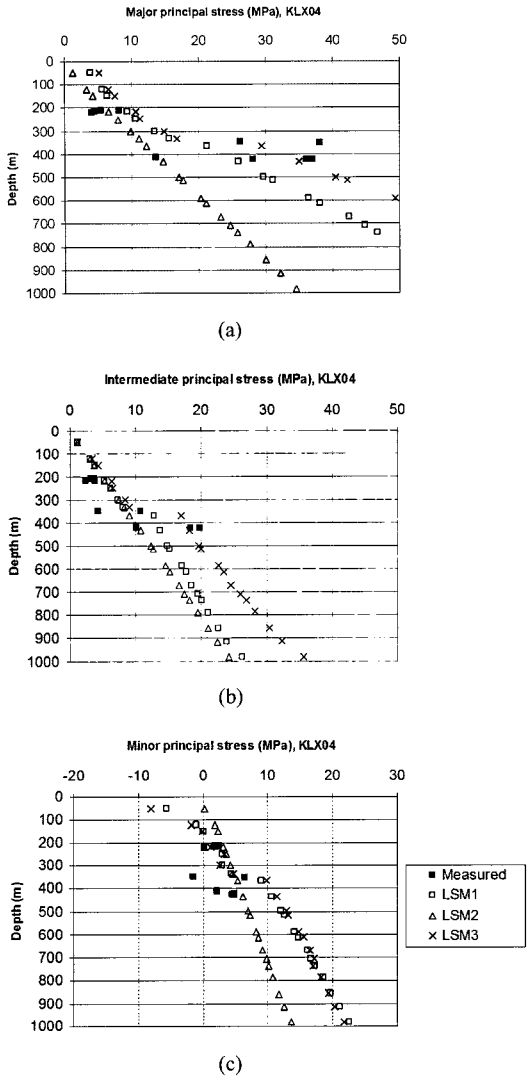

Fig. 10. Comparison between measured and modelled stresses at borehole KLX04. (a) Major principal stress; (b) Intermediate principal stress; and (c) Minor principal stress

local model (Figure 2), and rock stress was measured by the overcoring method. Borehole intersects deformation zone NE012A between 745 m and 947 m. Stress was measured above the intersection of the deformation zone, and it was generally low with no distinct change.

Figure 11 shows the modelled stress distribution along section BB' and, in general, the influence of NE012A is not evident. However, vertical deformation zone NE004A seems to affect the stress distribution. A slightly relaxed zone is generated due to the movement of deformation zone NE004A. Figure 12 shows the comparison between measured and modelled stresses at KLX04 for three different stress models. LSM 1 and LSM 3 generally overestimate the stress, while LSM2 fits relatively better. This is mainly due to the fact that the applied boundary stress is lower in LSM2.

The Äspö area is located in the northern part of the local model (Figure 2). A number of stress measurements were conducted in the area using both overcoring and hydraulic-fracturing methods. Within the depth considered in this study (< 1000 m), the area does not meet the large-scale deformation zone.

Figure 13 presents the comparison between measured and modelled stresses in the Äspö area. The extent of the scattering in the measured stress made it difficult to match with any of the suggested stress models, even though LSM 1 and LSM 3 seem to lie in the middle of the scattered measured stress values. As the quality of measured data varies significantly, refinement of the measured data may be necessary in order to make the comparison more effective.

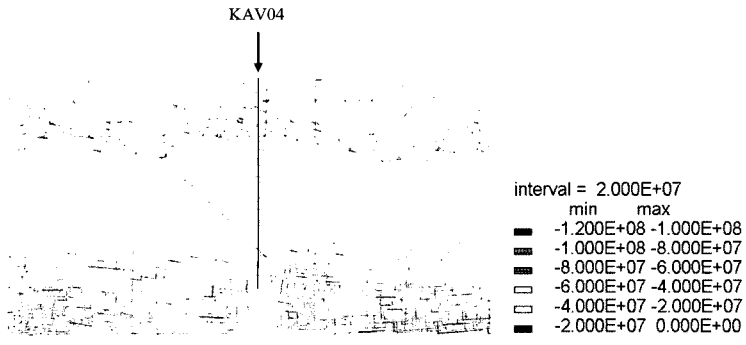

Fig. 11. Modelled stress distribution around borehole KAV04

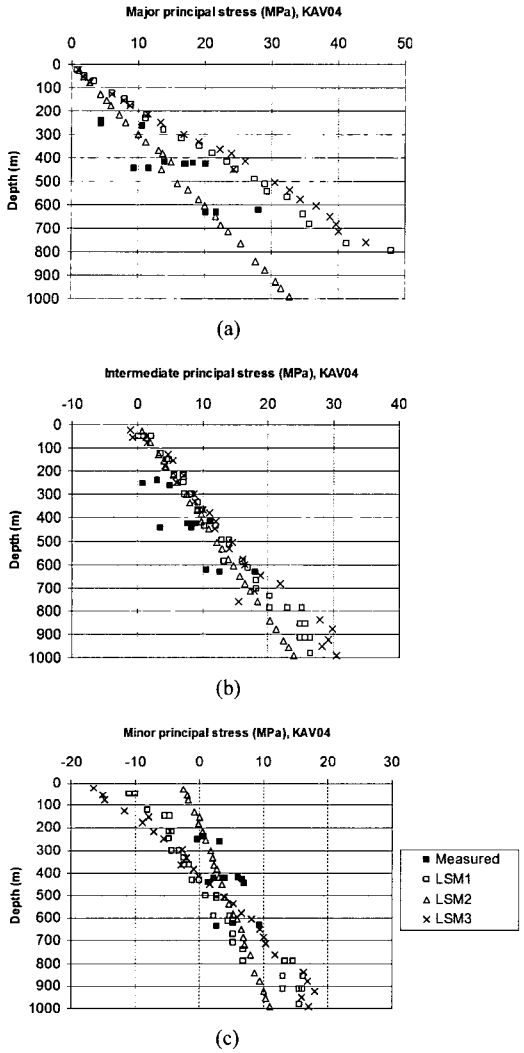

Fig. 12. Comparison between measured and modelled stresses at borehole KLX04. (a) Major principal stress; (b) Intermediate principal stress; and (c) Minor principal stress

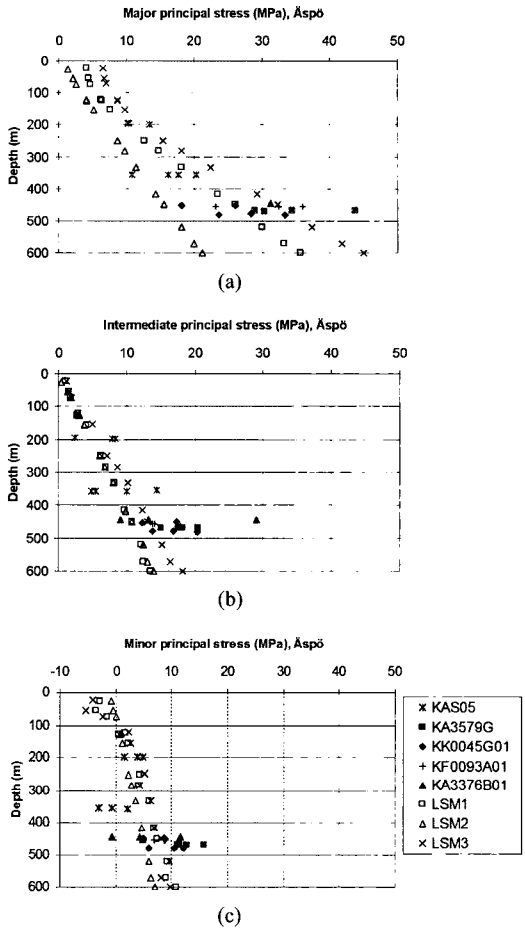

Fig. 13. Comparison between measured and modelled stresses at the Äspö area. The legend denotes different stress measurement campaigns. (a) Major principal stress; (b) Intermediate principal stress; and (c) Minor principal stress

4.2 Stress distribution in vertical and horizontal sections

Figure 14 presents the joint shear displacement in the vertical and horizontal sections in the local model. Deformation zones EW002A, EW007A and NE024A have the largest displacement, and their corresponding impacts on the stress distribution are anticipated. In general, vertical joints do not have large displacements along the joints due to the unfavorable stress direction with respect to the orientation of joints. Displacement along vertical deformation zones EW038A and NE004A (upper part) are relatively larger than other vertical deformation zones, because their directions are more favorable for sliding, which reconfirms the importance of the orientation of joint for the effect on the stress.

Figure 15 presents principal stresses along vertical sections AA', BB', and CC'. The results are plotted with respect to the entire length of the regional model, and boundary stresses are indicated. Note that the boundary stresses for intermediate and minimum principal stress are the same for LSM 3. Variation of stresses is due to the influence of the deformation zones and their interactions. In general, maximum principal stress decreases in wedge-type blocks that are confined by the intersecting deformation zones. Intermediate and minimum principal stresses show

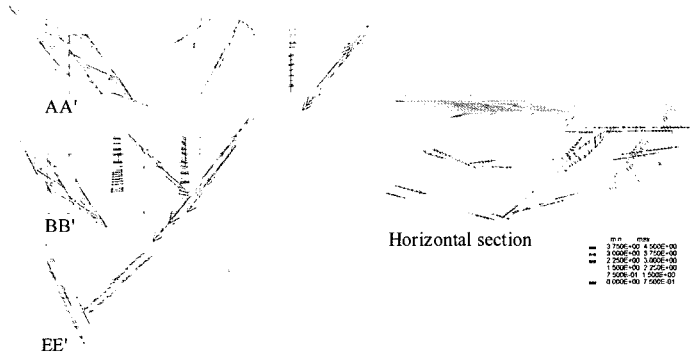

Fig. 14. Joint shear displacements in the local model in vertical and horizontal sections

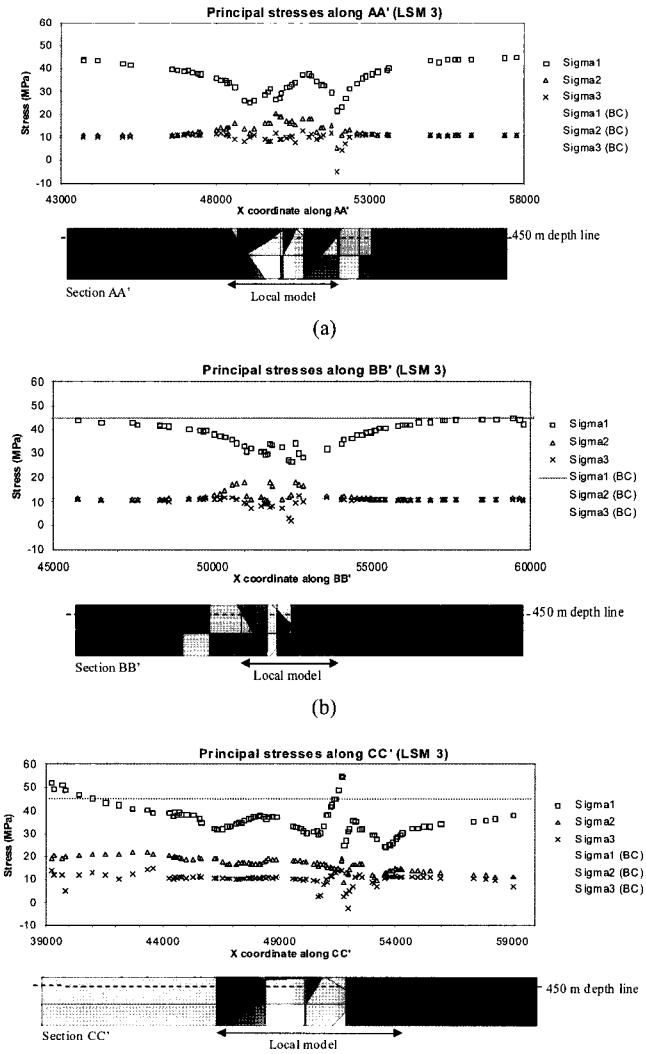

Fig. 15. Principal stresses along reference sections at 450 m depth (LSM 3). (a) section AA'; (b) section BB'; and (c) section CC'. The scales of graphs and sections views correspond. Note that Sigma 2 (BC) and Sigma 3 (BC) are identical for LSM model

relatively modest changes. In section AA', a distinct decrease of stress is observed in two locations. A decrease occurs at a wedge-type block formed by deformation zones EW002A and EW007A and near deformation zone NE024A. Between these two locations, a slight increase of intermediate principal stress is observed, which can be explained in view of stress equilibrium. In section BB', there is an overall decrease of maximum principal stress. In this section, the big wedge formed by deformation zones EW002A and NE024A is a clue for the explanation of the trend of the stress. In section CC', more fluctuation of stress is observed. Especially near the x-coordinate 52000, unusually high stress is observed due to the small wedge formed by NE012A and NE004A. Since this may be due to a lock up of the wedge, additional analysis with alternative geometry (GEO2) was performed and will be presented separately as a parametric study.

Figure 16 presents the stress distribution along horizontal sections at depths of 50 m and 450 m in the local model. At a depth of 50 m, there is a clear influence of fractures on the orientation of the principal stress. The influence on the orientation of the principal stress is more prominent at shallow depths than deeper depths because there is no overburden in the surface of the model that may promote the sliding of the fractures near surface. In terms of magnitude, stress is smaller along the major deformation zones, EW002A, EW007A, and NE004A. Stress concentration is found in the mid-south and south-west of the local due to abrupt termination of joints. It is not clear whether the *in situ* deformation zone has such an abrupt termination as modelled in this numerical study. If the termination of the deformation zone has a smoother end, the stress obtained in this study may be exaggerated and should be interpreted carefully.

4.3 Predicted stress at planned measurement campaign at KLX09 and KLX10

Prediction of stress is made on borehole KLX09 and KLX10, which are located below KLX06 on section DD' (Figure 2). These two boreholes are considered for a possible stress measurement study. Borehole KLX09 meets deformation zone EW007A,

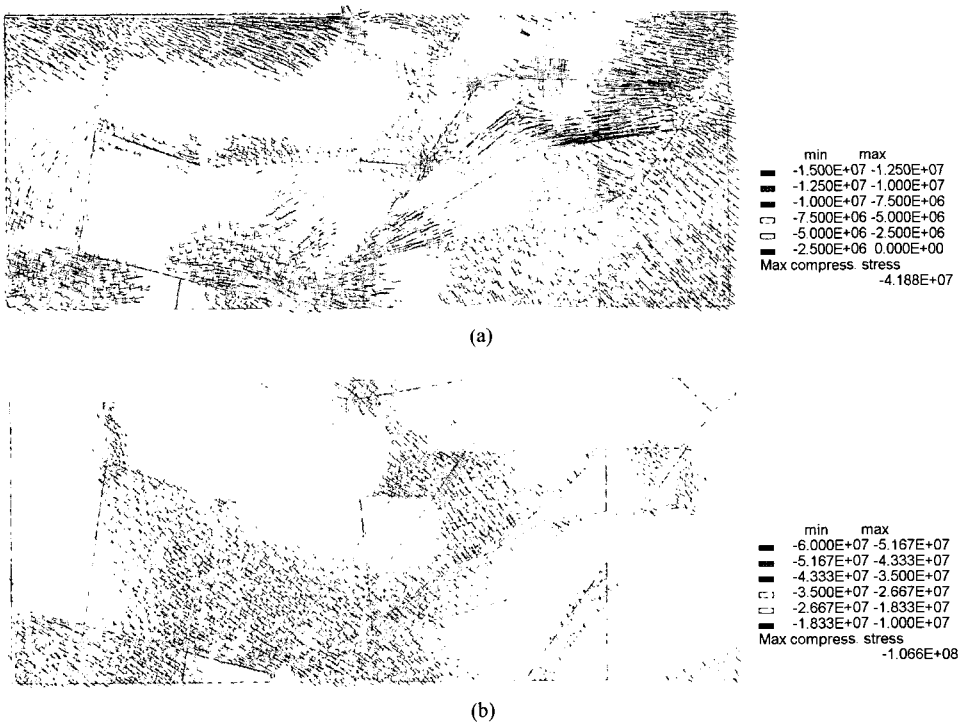

Fig. 16. Principal stress distribution along the horizontal section in the local model (a) 50 m depth and (b) 450 m depth

but KLX10 does not. Prediction by numerical modelling shows that stress at KLX09 will be generally lower than at KLX10. Figure 17 shows the distribution of principal stress along section DD' containing borehole KLX09 and KLX10, and the influence of deformation zone EW007A is evident. It is intended that the modelling results shown in this study can be used to assist in interpreting the stress data obtained during future stress measurement studies.

5. DISCUSSION

It is shown in this study that the degree of agreement between measured and modelled stresses varies significantly. While the numerical model successfully captured the variation of stress in borehole KLX04, comparisons with borehole KAV04 or the Äspö area only provide anecdotal evidence that numerical modelling may be useful. Some of the remaining issues and concerns are discussed here.

A possible extension of deformation zone NE012A to deformation zones NE018A and NE004A was examined with alternative geometry called GEO2. Figure 18 shows the section views for GEO2 that have different extensions of NE012A from the original model called GEO1. The marked circles indicate the differences from GEO1. As noted in Figure 18, the NE012 terminates against NE004 in GEO1, while it terminates against NE018A and NE024A in GEO2.

Principal stress along vertical section CC' shows that an anomaly in model GEO1 near x-coordinate 52000 that is not observed in model GEO2. This seems to suggest that the anomaly observed in GEO1 may be misleading, since such a large difference is hard to explain. Figure 19 shows the comparison of modelled stresses along section AA' and BB' between

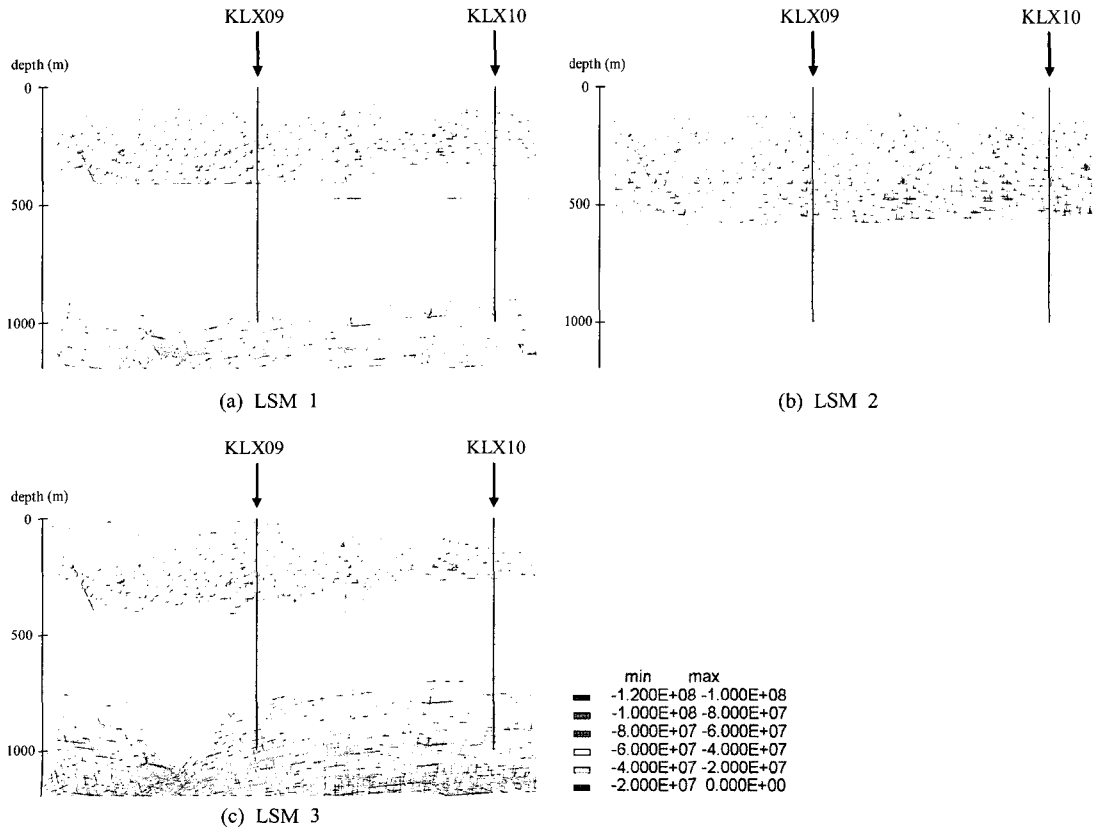

Fig. 17. Distributions of principal stresses along section DD'. Magnitudes and directions are indicated. (a) LSM 1; (b) LSM 2; and (c) LSM 3

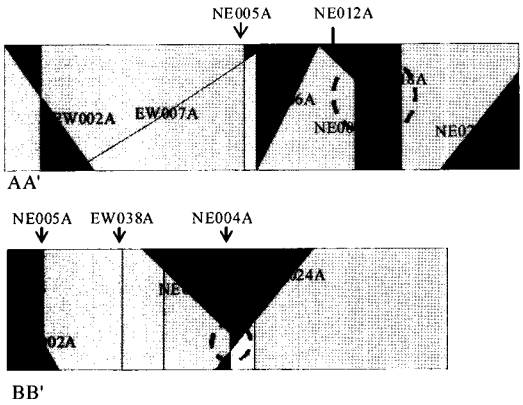

Fig. 18. Section view of the local model for GEO2. Section AA' and Section BB' are shown with circular marks that indicate the different area from GEO1

models GEO1 and GEO2. More stress relaxation is observed in model GEO2 in which the joint extends more, and larger joint displacement can occur.

Explicit representation of the deformation zone requires a very fine mesh in the numerical modelling, and this can require excessive computing time, especially for three-dimensional modelling. Since the minimum width of the deformation zone included in the modelling is 50 m, minimum mesh size needs to be in the order of tens of meters. Since the size of the local model is in the order of a kilometer, computing time for the model would be too severe, i.e., one calculation would take a few weeks with a modern personal computer. In order to avoid this severe computing time, deformation zones in this study were modelled as planar joints. Compared with the deformation zone, the planar joint has a distinct discontinuity, but it does not have a thickness. The friction angle of the deformation zone estimated from an empirical approach is about 40 degrees (SKB, 2004). The comparison study conducted by two-dimensional, distinct-element modelling shows that the extent of stress redistribution with an internal friction angle of 40 degrees for the deformation zone is achieved with a friction angle of approximately 20 degrees for a joint, and this provides support for the choice of a friction angle of 20 degrees used for this study (Hakami et al., 2006). Furthermore, it is necessary to consider the fact that pore pressure is not included in this purely mechanical analysis. As pore pressure will facilitate the sliding of

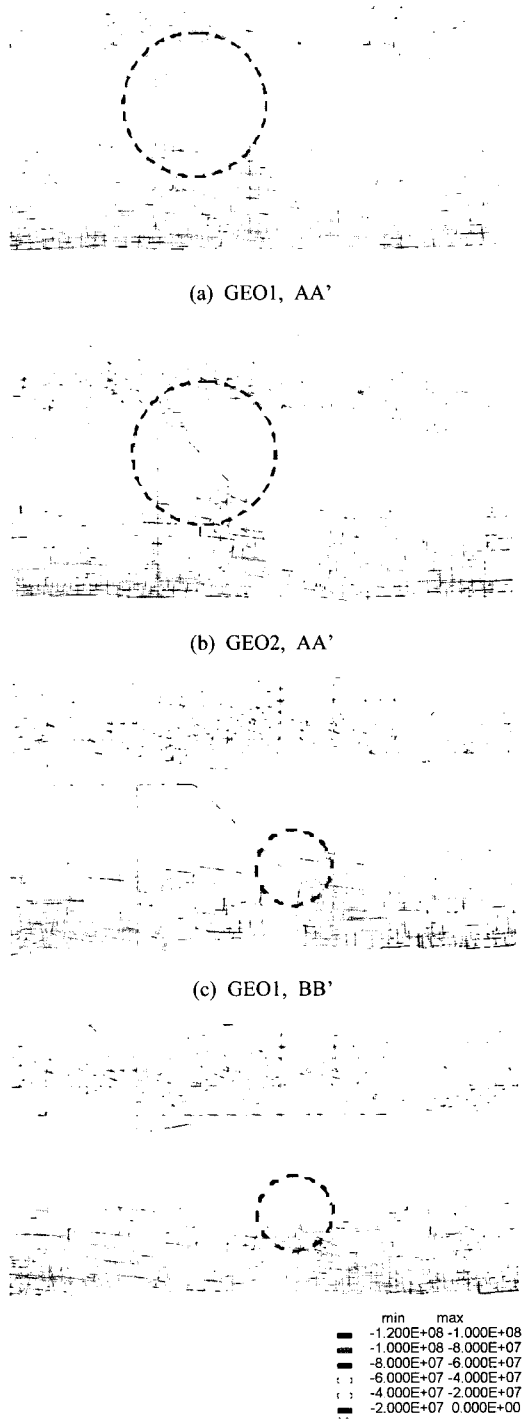

Fig. 19. Comparison of modelled stress along section AA' and BB' (near KAV04) between GEO1 and GEO2

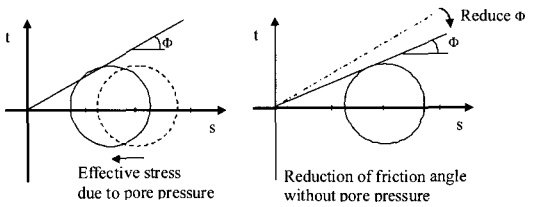

Fig. 20. Concept of reduction of friction angle for pure mechanical analysis

fractures, reduction of friction angle is necessary to consider this effect.

Given that the effect of topology is limited in the Oskarshamn area, the deformation zone is one of the most important factors that influences the state of stress significantly. The result of this study is dependent largely on the specific geological structures that were included in the geometry of the numerical model. With more detailed characterization regarding the geometry of the deformation zone and frictional properties of the fractures, the results of this study can be refined further. Such detailed characterization includes a more accurate characterization of the geometry and nature of the deformation zone, and this information may be used to assign different properties in each deformation zone.

This model did not simulate the tectonic history of the region, i.e., only the final state of stress is applied in the model. However, the current state of stress is the function of present-day tectonic load as well as the past loading path. Previous studies indicate that the state of stress can be different depending on the loading path (Brady et al., 1986; Homand et al., 1997). Locked-in stress can be generated due to the past loading history, and this adds to the complexity of the state of stress. According to a study of the geological evolution in the Oskarshamn region, the direction of principal stress direction changed a few times due to the crustal movement (SKB, 2004). For instance, the direction of principal stress was south, southwest, and west in different periods. It is plausible that such a change in the past could have an impact on the current stress state. The sequential modelling of tectonic history may be able to provide a useful clue to the explanation of the state of stress in relation to the tectonic history in the Oskarshamn area.

6. CONCLUSION

Three-dimensional numerical analysis was conducted to model the state of stress in the Oskarshamn area using the three-dimensional distinct element method. Far-field stress was applied on the geometrical model that represented the deformation zones as a planar joint. Measured and modelled stresses were compared in order to choose the numerical model that best fits the measured data. Main conclusions are summarized as follows:

1. The numerical model successfully captured the variation of measured stress observed at borehole KLX04 which showed a sudden increase in stress. This change was explained by the influence of the deformation zone EW007A and the modelled state of stress is closely related to the geometry of large-scale deformation zones identified in the region. The study shows that numerical analysis can be an effective tool in improving the understanding of the state of stresses in a geological formation.
2. The modelled stress at KAV04 slightly overestimated the measured stress, and this needs further investigation. The modelled stress at the Äspö area matched the measured stress only moderately. Discrepancies between measured and modelled stress are attributed to the inconsistent quality of measured stress, uncertainty in geological geometry, and input data for fractures.
3. A significant decrease of maximum principal stress was observed in the area where a wedge is formed. Stress release in the area can be explained by the formation of a wedge by a few intersecting, large-scale deformation zones. The change of stress is more significant when the large-scale fractures are more optimally oriented for sliding under the given *in situ* stress condition. The amount of change depends on the conditions that affect the sliding of fractures. The initial boundary condition of stress and the selection of frictional properties are most important factors that determine the state of stress with the given geometry of fractures.

ACKNOWLEDGEMENT

Special thanks are given to Dr. Eva Hakami of Itasca Consulting Group for initiating the project and for fruitful discussion. Financial support for the studies was provided by the Swedish Nuclear Fuel and Waste Management Company (SKB).

REFERENCES

1. Amadei, B. and O. Stephansson, 1997, Rock stress and its measurement, Chapman and Hall, London, 490p.
2. Bandis, S.C., A.C. Lumsden and N.R. Barton, 1983, Fundamentals of rock joint deformation, Int. J. Rock Mech. Min. Sci. & Geomech. Abstr. 20(6), 249-268.
3. Brady, B.H.G., J.V. Lemos and P.A. Cundall, 1986, Stress measurement schemes for jointed and fractured rock, In: Stephansson O. (ed), Rock stress and rock stress measurement, Luleå, Sweden, 167-176.
4. Fairhurst, C., 2003, Stress estimation in rock: a brief history and review, Int. J. Rock Mech. Min. Sci. 40 (7-8), 957-973.
5. Hakala, M., J.A. Hudson and R. Christiansson, 2003, Quality control of overcoring stress measurement data, Int. J. Rock Mech. Min. Sci. 40(7-8), 1141-1159.
6. Hakami, E., H. Hakami and R. Christiansson, 2006, Depicting a plausible in situ stress distribution by numerical analysis - examples from two candidate sites in Sweden, In: Lu, Li, Kjorholt & Dahle (eds), In situ Rock Stress, Trondheim, Norway, 473-481.
7. Hakami, E., H. Hakami and J. Cosgrove, 2002, Strategy for a Rock Mechanics Site Descriptive Model - Development and testing of an approach to modelling the state of stress, Svensk Kärnbränslehantering AB, SKB R-02-03.
8. Hart, R., 2003, Enhancing rock stress understanding through numerical analysis Int. J. Rock Mech. Min. Sci. 40(7-8),1089-1097.
9. Homand, F., M. Souley, P. Gaviglio and I. Mamane, 1997, Modelling natural stresses in the Arc Syncline and comparison with in situ measurements, Int. J. Rock Mech. Min. Sci. 34(7), 1091-1107.
10. Homberg, C., J.C. Hu, J. Angelier, F. Bergerat and O. lacombe, 1997, Characterization of stress perturbations near major fault zones: insights from 2-D distinct-element numerical modeling and field studies (Jura mountains), J. Structural Geology, 19(5), 703-718.
11. Hudson, J.A. and F.H. Cornet, 2003, Special issue on rock stress estimation, Int. J. Rock Mech. Min. Sci. 40(7-8), 955.
12. Itasca Consulting Group Inc., 2003, Three Dimensional Distinct Element Code - User's Guide, Minneapolis, Minnesota, USA.
13. Martin, C.D. and N.A. Chandler, 1993, Stress heterogeneity and Geological structures, Int. J. Rock Mech. Min. Sci. 30(7), 993-999.
14. Min, K.B., C.I. Lee and H.M. Choi, 2003, An experimental and numerical study of the in-situ stress measurement on transversely isotropic rock by overcoring method, In: Sugawara K et al (eds), 3rd International Symposium on Rock Stress - RS Kumamoto '03, Kumamoto, 189-195.
15. Pollard, D.D. and P. Segall, 1987, Theoretical displacements and stresses near fractures in rock: with applications to faults, joints, veins, dikes, and solution surfaces, In: Atkinson B.K. (editor), Fracture mechanics of rock, Academic Press Inc, London, 277-349.
16. SKB, 2004, Preliminary site description, Simpevarp area - version 1.1, Svensk Kärnbränslehantering AB, SKB R-04-25.
17. SKB, 2006, Preliminary Site description. Laxemar area - version 1.2, Svensk Kärnbränslehantering AB, SKB R-06-10.
18. SKB, 2007, RD&D Programme 2007, Programme for research, development and demonstration of methods for the management and disposal of nuclear waste, Svensk Kärnbränslehantering AB, SKB TR-07-12.
19. SKB, 2007, Forsmark site investigation, Programme for long-term observations of geosphere and biosphere after completed site investigations, Svensk Kärnbränslehantering AB, SKB R-07-34.
20. Su, S and O. Stephansson, 1999, Effect of a fault on in situ stresses studied by the distinct element method, Int. J. Rock Mech. Min. Sci. 36(8), 1051-1056.

민 기 복

1994년 서울대학교 자원공학과 공학사
1999년 서울대학교 자원공학과 공학석사
2004년 스웨덴 왕립공과대학 (Royal Institute of Technology) 공학박사

Tel: 061-8-8303-6471
E-mail: ki-bok.min@adelaide.edu.au
현재 호주 애들레이드 대학교 토목환경자원공학부 조교수